Liang et al. Journal of Biological Engineering (2023) 17:39
https://doi.org/10.1186/s13036-023-00355-7

Journal of Biological Engineering

REVIEW

Open Access

Advances in the application of Mxene nanoparticles in wound healing

Chengzhi Liang[1†], Jing He[2†], Yuan Cao[1†], Guoming Liu[1], Chengdong Zhang[1], Zhiping Qi[3], Chuan Fu[4*] and Yanling Hu[1*]

Abstract

Skin is the largest organ of the human body. It plays a vital role as the body's first barrier: stopping chemical, radiological damage and microbial invasion. The importance of skin to the human body can never be overstated. Delayed wound healing after a skin injury has become a huge challenge in healthcare. In some situations, this can have very serious and even life-threatening effects on people's health. Various wound dressings have been developed to promote quicker wound healing, including hydrogels, gelatin sponges, films, and bandages, all work to prevent the invasion of microbial pathogens. Some of them are also packed with bioactive agents, such as antibiotics, nanoparticles, and growth factors, that help to improve the performance of the dressing it is added to. Recently, bioactive nanoparticles as the bioactive agent have become widely used in wound dressings. Among these, functional inorganic nanoparticles are favored due to their ability to effectively improve the tissue-repairing properties of biomaterials. MXene nanoparticles have attracted the interest of scholars due to their unique properties of electrical conductivity, hydrophilicity, antibacterial properties, and biocompatibility. The potential for its application is very promising as an effective functional component of wound dressings. In this paper, we will review MXene nanoparticles in skin injury repair, particularly its synthesis method, functional properties, biocompatibility, and application.

Keywords MXene, Wound dressing, Nanoparticles, Wound healing

Introduction

Cutaneous wound healing is a precise and complex process which involves multiple immune cells, non-immune cells, cytokines, growth factors, and extra cellular components [1]. The normal wound healing process can be categorized by four phases: (a) Hemostasis (b)inflammation, (c) proliferation and (d) remodeling, or three phases by considering the hemostasis/inflammation phase as one phase [2, 3]. Although these phases are interrelated, they have different processes. The first stage of wound repair are hemostasis and inflammation, which occurs immediately after tissue injury. The inflammatory pathways are thus activated, and the immune system works to remove inactivated tissue to prevent infection. It also activates the clotting cascade and promotes clotting to prevent continuous fluid loss. At the same time, the fibrin clot formed in the process of blood coagulation can be

†Chengzhi Liang, Jing He and Yuan Cao have equalcontribution to this work and should be considered as co-frst authors.

*Correspondence:
Chuan Fu
fuchuan2015@163.com
Yanling Hu
huyanlingqy@126.com
[1] Department of Orthopedic Surgery, The Affiliated Hospital of Qingdao University, Shandong 266000, PR China
[2] Department of Pediatric Surgery, The Affiliated Hospital of Qingdao University, Shandong 266000, PR China
[3] Department of Orthopedic Surgery, The Second Hospital of Jilin University, Chuangchun 130041, China
[4] Key Laboratory of Molecular Medicine and Biotherapy in the Ministry of Industry and Information Technology, Department of Biology, School of Life Science, Beijing Institute of Technology, Beijing 100081, PR China

used as a barrier to prevent foreign bacteria from invading the human body through skin damage [1, 3]. Most conventional wound dressings address this first phase of skin repair in order to promote wound healing by absorbing exudate, maintaining a moist local environment, and preventing infection. The second stage of wound repair is proliferation. This process takes place between 2 and 10 days after tissue injury, and it involves angiogenesis, granulation tissue formation, and synthesis of extracellular matrix (ECM) components. In this phase, Cytokines such as vascular endothelial growth factor A (VEGFA) and fibroblast growth factor 2 (FGF2/bFGF) are secreted in large amounts in the wound, which helps to accelerate wound healing. Additionally, in this second stage, fibroblasts and myofibroblasts work together to produce extracellular matrix. Appearing as collagen, it eventually forms mature scars [4]. The third stage of wound repair is remodeling. This phase occurs around 2–3 weeks after the initial injury and lasts for about a year or more. During this stage, most macrophages and myofibroblasts will gradually apoptosis. Meanwhile, the extracellular matrix is gradually reconverted from a type III collagen backbone to a type I collagen backbone [5]. The entirety of the skin repair process shows that there are several factors involved in the process of wound healing.

Throughout this process, many external factors can hinder the healing of the wound. Currently, infection and endogenous growth factor deficiency are considered as the two main factors that affect skin healing. The wound healing process is typically characterized by bacterial infections, which can lead to increased exudate from the wound site and can inhibit granulation tissue formation, which thereby prevents wound healing [6]. Antibiotics are widely accepted as an effective means to prevent and treat wound infections; however, the misuse and abuse of antibiotics eventually leads to bacterial resistance, which thereby reduces its therapeutic efficacy [7, 8]. Inadequate endogenous growth factors are another factor that can affecting wound healing, as they are incapable of effectively responding to local injuries, thus interfering with normal biological pathways and inflammatory responses. Ultimately, this results in delayed wound healing [9]. Traditional dressings such as gauze only play passive roles in the healing process, such as shielding, moisturizing, absorbing exudate, and preventing injury from external stimuli [10]; however, they rarely impact antimicrobial or active regulation of endogenous factors to promote wound healing. Therefore, the new dressing strategy suggests loading the traditional dressings with active substances or combining them with other therapeutic approaches to accelerate the healing process (as shown in Fig. 1). Currently, one of the most widely adopted approaches is to load dressings with active substances that have natural bactericidal properties and actively modulate endogenous related cells and factors. This method improves the antimicrobial and tissue repair capacity of the dressing [11]. A wide variety of bioactive agents have been used in the preparation of wound dressings as a way to increase their antimicrobial properties and modulate endogenous growth factor production; this is summarized in Table 1.

Among the array of active agents, MXene have come to the forefront in recent years thanks to its unique structure and physicochemical properties. MXene are a novel family of two-dimensional (2D) materials which are made up of transition metal carbides, nitrides, or carbon-nitrides [21]. They can be calculated with the general formula $Mn^{+1}Xn$, where M represents transition metals (e.g., Sc, Ti, Cr, etc.) and X is carbon and/or nitrogen [22]. MXene are synthesized as a result of etching from the MAX phase. This is a layered ternary carbide and nitride with the general formula $Mn^{+1}AXn$, where A represents periodic table of elements groups 13 and 14 (as shown in Fig. 2). MXene possess many unique physicochemical properties, for example: (a) MXene have hydrophilic functional groups on their surface (-OH, -O, etc.), which gives them an advantage as they do not require complex surface modification compared to other hydrophobic nanoparticles [23]; (b) MXene possess high metallic conductivity [24, 25]; and (c) MXene have excellent biocompatibility [26], allowing

Table 1 Commonly active agents loaded in wound dressings and characteristics

Active agents	Characteristics	Reference
Ag NPs	Antibacterial properties, low toxicity, modulate anti-inflammatory, cytokine release reduced penetration into the skin.	[12, 13]
Au NPs	Antibacterial properties, low toxicity, stimulated angiogenesis and fibroblast proliferation.	[14, 15]
ZnO NPs	Antibacterial properties, low toxicity, formation of hemostatic blood clots.	[16]
Flivasorb	Absorb the exudate and retain it firmly within the dressing.	[17]
Chitosan	High bioavailability and low toxicity, antibacterial properties.	[18]
Nanocellulose	High surface area per unit, increased biocompatibility, hydrophilicity and nontoxicity, damp environment	[19]
Gelatin	Biodegradable, highly biocompatible, non-immunogenic.	[20]

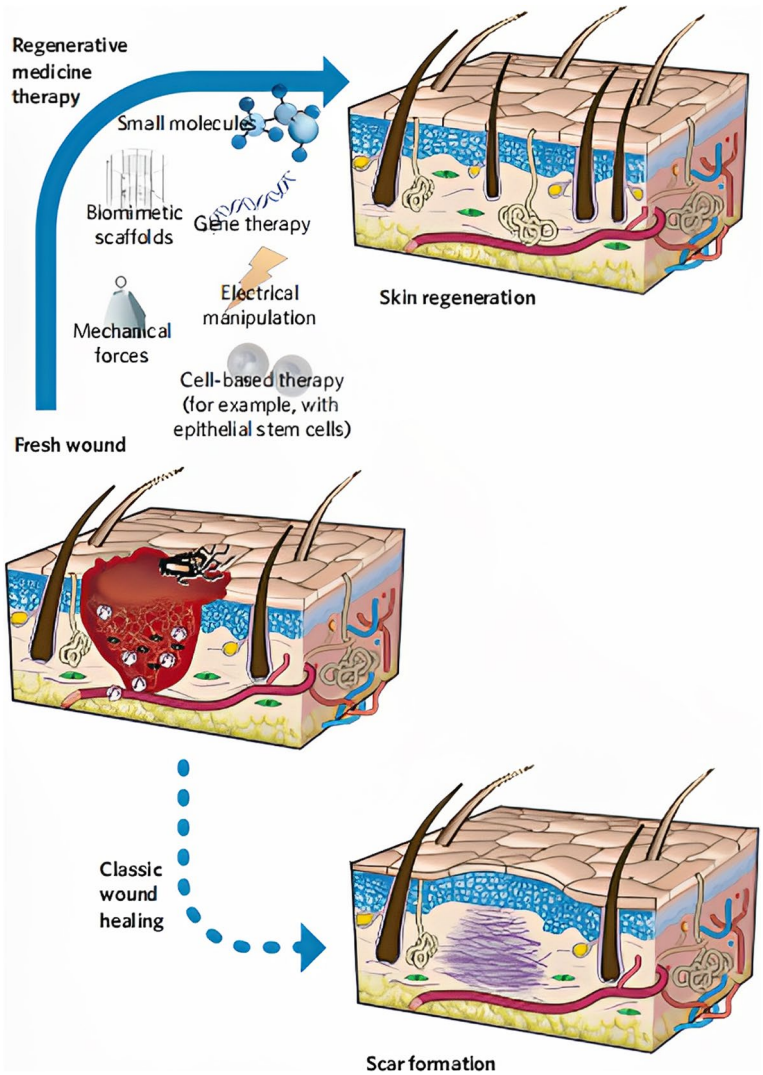

Fig. 1 Innovative dressing strategies that promote wound healing include bionic scaffolds, electrically stimulated environments, loaded small molecules, gene therapy, and stem cells [1]

it to be removed and degraded in vivo [27]. Considering the above advantages, MXene have attracted extensive research interest in the field of nanomedicine. It has also been widely used in the preparation of wound dressings in recent years. In this paper, we summarized the recent developments of MXene nanoparticle composite wound dressings as well as their application prospects in wound healing. Furthermore, we analyzed their current opportunities and challenges in wound healing.

Materials and methods

References with sturdy pages "Wound healing", "Wound dressing", "MXene" and nanoparticles "were indexed in PubMed and Web of science. The period of retrieval is mainly from 2015 to now.

The synthesis of MXene

MXene synthesis can be presented as two methods: bottom-up synthesis and top-down synthesis. Choosing the suitable method for synthesis is crucial for the physicochemical properties of the synthesized products, such as the size, morphology, and function of the material [29]. The synthesized MXene can be further modified on the surface to enhance their biocompatibility for enhanced biomedical applications. Currently, the top-down synthesis from the MAX phase is the one that is most widely used.

Top-down approach

The top-down synthesis method has two steps: the etching of the MAX phase and the delamination of MXene.

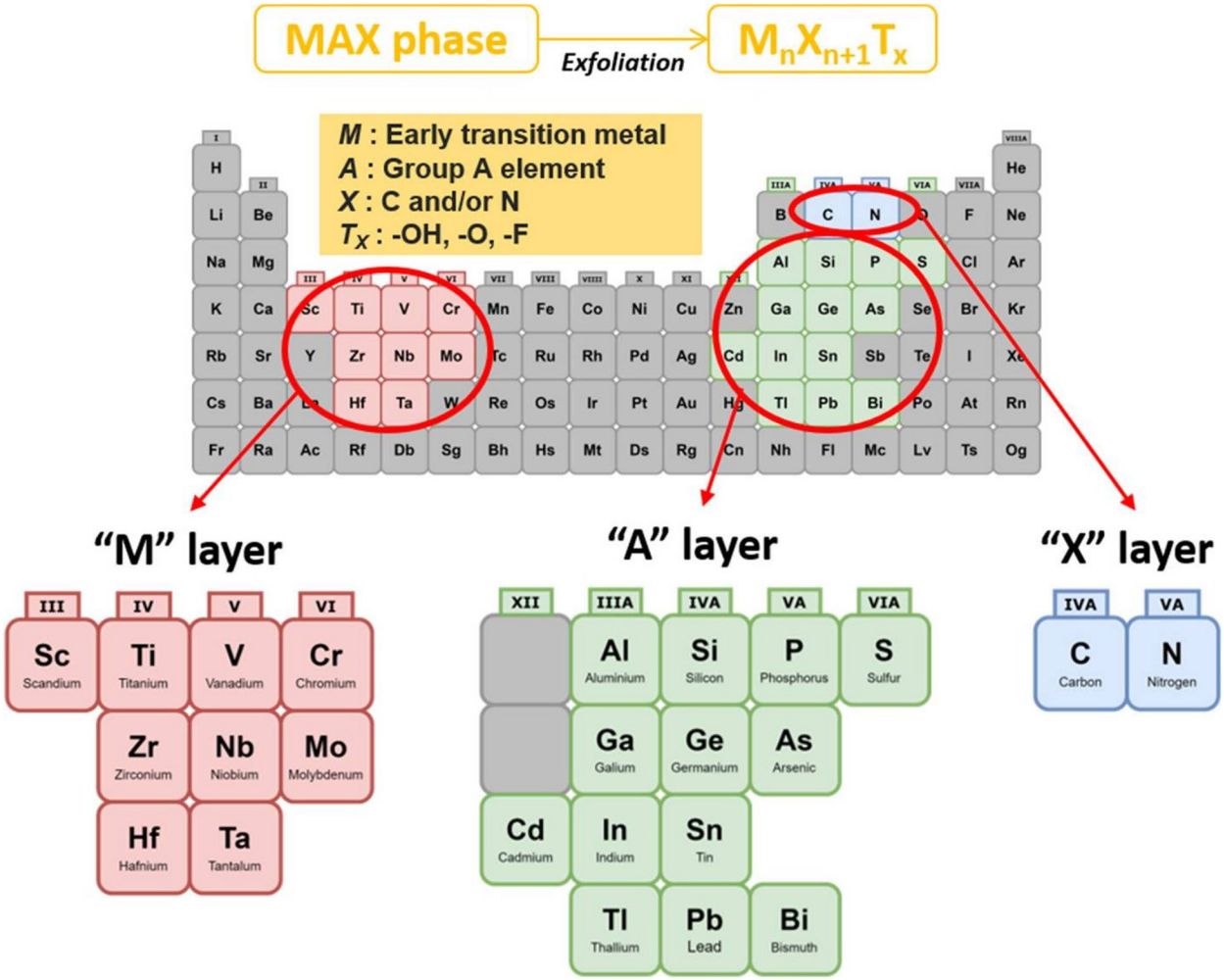

Fig. 2 General element composition of MAX phase and MXene [28]

The etching of the MAX phase is the process of synthesizing MXene by wet chemical etching of the MAX phase with hydrofluoric acid (HF) or HF-containing etchant or the in situ formation of HF, like removing the A element from the MAX phase ($Mn^{+1}AXn$) or the etching of Al in Ti_3AlC_2. In the MAX phase, there is a strong chemical bond between the A and M elements, making it difficult to remove them mechanically. Therefore, it is necessary to obtain MXene by selective etching with etchant in order to remove the ionic bonds. For the synthesis of MAX phase, Ti_3AlC_2 MAX phase (precursor of $Ti_3C_2T_x$) was used as an example. Ti_3AlC_2 can be synthesized by putting different raw materials under different conditions. Prior to our current understanding, a mixture of Ti_2AlC and TiC was used to synthesize Ti_3AlC_2 [30]. However, thanks to the development of technology, the use of cheaper raw materials (TiC, Ti, and Al) for the synthesis of Ti_3AlC_2 [31] emerged. Also, the mixtures of Ti, Al, and C [32], Ti, Al_4C_3, and C [32], and TiO_2, Al, and C [33] have all been reported for the synthesis of Ti_3AlC_2. In addition to the aluminum-attached MAX phase in the above examples, some other ion-linked MAX phase precursors, such as $Mn^{+1}GaXn$, $Mn^{+1}SiXn$ [29], can also be used for the preparation of MXene.

Firstly, etching is performed. Concentrated HF was the preferred etchant for selective removal of Al from Ti_3AlC_2 as reported in the literature [30]. The Max phase precursor (Ti_3AlC_2 powder) can be selectively etched off Al by immersing it in 50% HF at room temperature for two hours. However, high concentrations of HF have a high toxicity, which can induce cell death [29], cause systemic toxicity, and even cause death [34]. Therefore, many scholars are studying ways to effectively avoid using high concentrations of HF in the preparation process. One study compared three different concentrations of HF at 30%, 10%, and 5%. Its findings revealed that only 5% HF could effectively remove Al [31], which suggests that diluted etching reagents can be used in replacement

of high concentrations of HF, in order to mitigate the toxic effects. Hydrogen fluoride salts, such as NH_4HF_2 [30, 35] and lithium fluoride (LiF), can be used for in situ preparation of HF for etching [24]. Although the properties of MXene prepared by in situ HF etching are similar to those of HF synthesis, it prevents the hazardous effects of HF toxicity during the synthesis process. Meanwhile, the prepared MXene is a monolayer structure, allowing for easy access to the next application.

In addition to HF etching or in situ formation of HF, it is possible to replace the "A" element in the MAX phase with other elements under high temperature conditions. For the reaction between Al-based MAX phase and $ZnCl_2$ at 550 °C, Al can be replaced by Zn to obtain a Zn-based MAX phase. And when there is an excess of $ZnCl_2$, Ti_2CCl_2 and $Ti_3C_2Cl_2$ can be obtained. Therefore, various MXene variants can be prepared via redox reactions [36]. Studies have also reported the application of non-MAX phase precursors to prepare MXene, which can also be produced from HF treatment using layered ternary $Zr_3Al_3C_5$ materials instead of the MAX phase as detailed here [37]. Table 2 summarizes the various methods and appropriate conditions of etching as described in this section.

After the selective removal of Al atoms through HF etchant, the second step is performed: delamination of MXene. The Ti_3C_2 layer is sonicated to terminate the top and bottom Ti layers in functional groups (Tx) such as O^{2-}, OH^- or F^- (Fig. 3). However, the resulting MXene thin films often have defects which affect the material's properties. The application of intercalating agents such as dimethyl sulfoxide (DMSO), tetrabutylammonium hydroxide (TBAOH), etc. prior to sonication can widen the interlayer spacing of MXene [23], making them easier to delaminate, and forming pure MXene thin films. Moreover, not only can intercalation compounds be used for the aforementioned purpose, it can also weaken the interactions between the 2D layers and delaminate MXene into separate 2D films. Another focus of research has been the preparation of MXene by using the minimum intensity layer delamination (MILD) method, which does not require sonication and uses a milder route to produce thin flims with larger but fewer defects [23]. An optimized MILD synthesis method using (12 M LiF/9 M HCl) at room temperature has also been reported [31]. Based on the current studies on the top-down synthesis of MXene, etchant selection, etching time, and type of intercalator are key parameters to ensure the successful synthesis of biocompatible MXene nanosheets.

Bottom-up approach

Bottom-up synthesis usually starts with small organic/inorganic molecular/atomic structures which undergo a crystal growth process to obtain 2D structures [23]. This has been studied [39] from the perspective of applying the chemical vapor deposition (CVD) technique to synthesize molybdenum carbide (Mo2C), which uses methane (CH4) and copper/molybdenum (Cu/Mo) foil at a temperature of 1085 °C or higher. High-quality, thin, and large nanosheets with few defects can be obtained by using this technique. However, due to the lack of functional groups on the nano-surfaces as well as the difficulty in penetrating into cells of this bottom-up method, at present, it can be deemed unsuitable for large-scale biomedical applications. In addition to CVD, existing literature details the synthesis of MXene [40] using methods such as the template method and plasma-enhanced pulsed laser deposition (PEPLD), such as 2D nitrides (MoN, V2N and W2N) [41]. Such bottom-up synthetic processes allow precise manipulation of the size distribution, morphology, and surface termination of MXene.

Table 2 Methods and conditions of etching

MAX Phase	Etching solution and condition	Resulting product	Characteristic	Reference
Ti_3AlC_2 powder	50%HF, room temperature, 2 h	Ti_3C_2	High toxicity	[23]
Ti_3AlC_2 powder	30%HF, room temperature, 5 h 10%HF, room temperature, 18 h 5%HF, room temperature, 24 h	Ti_3C_2Tx	Low toxicity	[31]
Ti_3AlC_2 powder	1 M NH4HF2, 60℃,8 h	Ti_3C_2	Non-toxic, monolayer MXene	[30, 35]
Ti_3AlC_2 powder	LiF + 6 M HCl, 35℃,24 h	Ti_3C_2Tx	Non-toxic, monolayer MXene	[24]
Ti_3AlC_2 powder	LiF + 9 M HCl, room temperature,24 h	Ti_3C_2Tx	Non-toxic, monolayer MXene	[31]
Ti_3AlC_2 powder	ZnCl2, 550℃	Ti_2CCl_2 $Ti_3C_2Cl_2$	Non-toxic, Need not MAX Phase	[36]
$Zr_3Al_3C_5$ powder (not MAXphase)	50%HF, room temperature	Zr_3C_2	Non-toxic, Need not MAX Phase	[37]

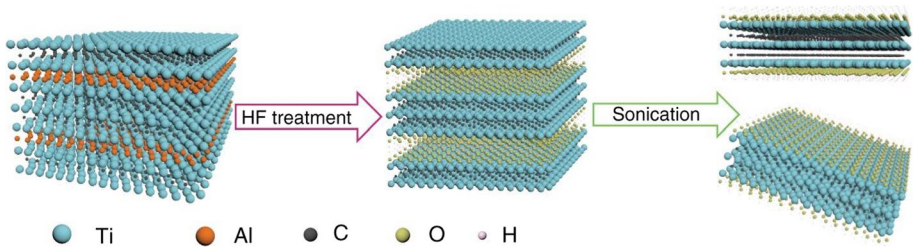

Fig. 3 Schematic diagram of the preparation of MXene by acid etching (taking Ti3C2Tx as an example) [38]

This precision concerning the surface termination is crucial for determining the product's properties and, consequently, its applications. Therefore, although there are few successful cases, this bottom-up approach to synthesis is still expected to be expanded in the future.

The property of MXene

MXene possess a set of excellent properties, notable among which are its hydrophilicity [21, 36, 42, 43], antimicrobial [44, 45] and photothermal features [44, 46, 47], electrical conductivity [23–25, 48, 49], and good biocompatibility [26, 27]. As shown in Fig. 4, these properties are the basis for why they are highly suitable as skin repair materials. Additionally, MXene has more hydrophilic groups compared to other 2D materials, meaning they are easier to functionalize by surface modification, and, thus, easily used in biomedical applications.

Antibacterial property

The antibacterial efficiency of Ti_3C_2Tx against gram-negative *Escherichia coli* and gram-positive *Bacillus subtilis* was higher than that of graphene oxide (GO), while the quantified extent of its antibacterial activity was dose dependent [44]. As revealed by SEM and TEM, in the absence of Ti_3C_2Tx, no cell damage or death was observed in cultured *E. coli* and *B. subtilis*. But when the Ti_3C_2Tx was present, varying degrees of cell damage could be seen in most bacterial cultures. It was also found the LDH release of both bacteria increased and the number of colonies decreased as the concentration of Ti3C2Tx was raised [44]. Shamsabadi et al. [45] investigated the antibacterial performance of four sizes of MXene nanosheets against *E. coli* and *B. subtilis* in dark conditions to exclude the photothermal effect of MXene nanoparticles themselves. It was discovered that the nanosheets showed bacterial DNA leakage and bacterial cell dispersion within 3 h [45]. In addition to the observational description of this antimicrobial phenomenon, Jastrzebska et al. systematically studied the structures of it [50] and the relationship between the atomic structures of Ti_2C and Ti_3C_2 MXene and their antimicrobial properties. Their work yielded the conclusion that there were no differences between Ti_2C and Ti_3C_2 MXene in terms of surface chemistry. However, Ti_2C MXene did not affect bacterial survival, while Ti_3C_2 MXene exhibited antibacterial properties. This result was posited to be caused by

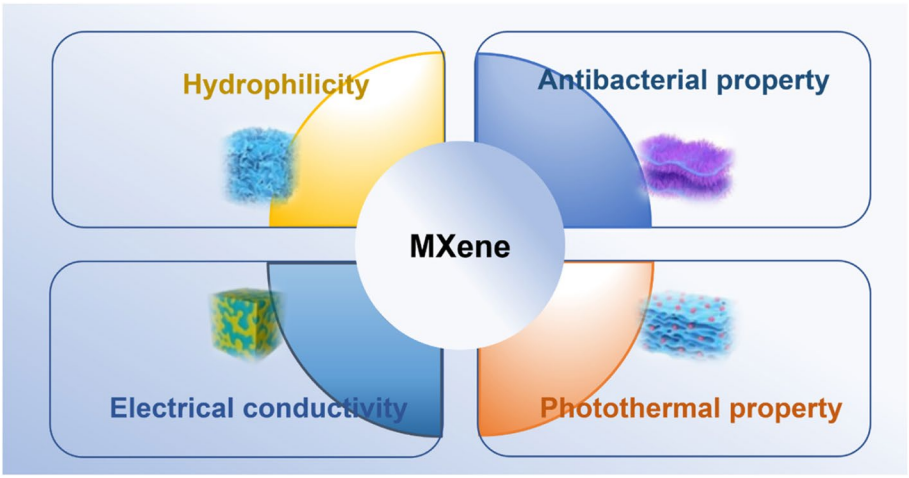

Fig. 4 Schematic diagram of the characteristics of MXene

the fact both have the same chemical composition at the atomic scale but different stoichiometry. In addition to inhibitory effects on commonly encountered bacteria, MXene were found to have inhibitory effects on fungi. As such, Lim et al. [51] focused upon the antifungal properties of Ti_3C_2Tx MXene, using inverted contrast microscopy to show how a large number of mycelium and spores were found in the control group without MXene. Conversely, fungal growth inhibition was observed in the experimental group treated with delaminated Ti_3C_2Tx (d-Ti_3C_2Tx) MXene, which led the authors to conclude d-Ti_3C_2Tx MXene nanosheets achieved such an outcome through disrupting the fungal hemispheric structure. Therefore, the d-Ti_3C_2Tx MXene nanosheets developed in this project may be a promising antifungal material which provide the basis for future research into promoting healing in infected wounds. All of the abovementioned research has shown MXene possesses good antibacterial properties and has a great deal of potential in the application of healing injuries. A considerable number of scholars have already prepared composites, with other materials serving as excipients, for the purpose of application to wounds. Table 3 summarizes the antibacterial property discussed above.

Photothermal performance

Existing literature reported Ti_3C_2's properties of 100% photothermal conversion efficiency and 84% photo-water evaporation efficiency when exposed to one solar irradiation (1 kW/m^2), which indicates MXene is a promising solar photothermal material [47]. The study also confirmed Ti_3C_2 nanosheets exhibit high near-infrared absorption and photothermal conversion efficiency under near-infrared laser irradiation (808 nm), as well as good biocompatibility [47]. In addition to Ti_3C_2, other MXene materials have similar properties, with Nb2C NS exhibiting very high photothermal conversion efficiency (36.4% at NIR-I and 45.65% at NIR-II) and high photothermal stability [27], while Ta_4C_3 nanosheets were found to have excellent photothermal conversion performance (efficiency η of 44.7%) [52]. All these studies indicate that, because of their excellent photothermal properties, MXene materials are a new photothermal agent with many application potential.

Electrical conductivity

The electrical conductivity of MXene is primarily dependent upon their constituent components. Components such as Nb_2C, Nb_2CF_2, etc. are metallic materials which exhibit semiconductor properties after surface modification [53, 54], and exhibit conductivity naturally. The structure of a single Ti_3C_2 layer is also similar to that of a semimetal which has been measured to be ≈0.03 μΩ m [55], and its low resistivity is a great advantage for biomedical applications. The conductivity of Ti_3C_2Tx can reach 6500 S cm-1 [25], and experiments demonstrated the band gap can be adjusted by changing its surface termination to improve the conductivity. Thereafter, 2D materials with high mobility and proper band gap could be obtained [56]. The conductivity of MXene has been studied extensively [23–25, 48, 49], and it has been used in applications including SMC electrodes, sensors, electronic devices, aerospace, and biomedical applications [57].

Hydrophilicity

MXene exhibit strong hydrophilicity [29, 58–60] due to the presence of a large number of hydrophilic functional groups (e.g., hydroxyl, oxygen, or fluorine) on the material's surface [21, 42, 43, 61]. These groups eliminate the need for complex surface modifications compared to other hydrophobic nanoparticles for biomedical applications [62]. This property, coupled with the unique surface terminations, enhance MXene's adaptability, and those which are modified can fully exploit its properties when introduced into other composite systems such as hydrogels.

The biocompatibility of MXene

MXene are widely used in various fields of research thanks to their unique features, but biocompatibility is a topic which cannot be avoided when exploring their biomedical applications. Biocompatibility is the most critical parameter for the evaluation of a material's potential for biomedical use, without which there is

Table 3 Antibacterial property

MXene	Experimental method	Result	Reference
Ti3C2Tx	Observe bacterial cell damage	LDH release and the number of colonies decreased	[44]
Ti3C2Tx	Observe bacterial in dark	Bacterial DNA leakage and bacterial cell dispersion	[45]
Ti2、Ti3C2	Observe the atomic structure and antibacterial activity	Ti2C MXene did not affect the survival of bacteria while Ti3C2 MXene showed antibacterial properties	[50]
d-Ti3C2Tx	Observe the growth of fungi	Fungal growth inhibition was observed in the d-Ti3C2Tx group	[51]

no basic condition for application. The specific surface area and ability to self-charge make it possible to control MXene's properties via surface modification [63]. Therefore, approaches to improve biocompatibility through surface chemistry using polymeric materials, biomolecules, or various other substances have been of interest to many scholars [64]. This section will be discussed in three parts: in vitro studies; in vivo studies; and improving biocompatibility.

In virto

In vitro experiments have found that MXene is more toxic to cancer cell lines. An article exploring the effect of MXene (Ti_3C_2) on the biological activity of two normal cell lines (MRC-5 and HaCaT) and two cancerous (A549 and A375) cell lines showed optimal cytocompatibility with HaCaT. In addition, MXenes had a higher toxic effect on cancer cells compared to normal cells, while cell viability decreased with the increase of Ti_3C_2 concentration. The study also suggests that oxidative stress may be a potential mechanism for MXene's toxic effects [50]. Szuplewska et al. [65] conducted an in vitro evaluation of the biocompatibility of Ti_2NTx from four types of cells: human skin malignant melanoma cells, human immortalized keratinocytes, human breast cancer cells, and normal human mammary epithelial cells. Their experiment concluded similarly with Jastrzebska [38] that MXene is more toxic to cancer cell lines than normal cell lines. Many studies have found MXene having significant dose-dependent toxicity, Wu et al. [66] used NSCs-derived cells and primary neural stem cells to study the cytotoxicity of Ti_3C_2 nanosheets, TEM results showed that at a dose of 12.5 μg/ml, Ti_3C_2Tx nanosheets had no observed adverse reactions to NSCs or NSCs-derived cells, and when the concentration was greater than 25 μg/mL, Ti3C2 nanosheets were internalized in neural stem cells with significant cytotoxicity. Jiang et al. found that high doses of Ti_3C_2Tx nanosheets (> 50 $\mu gmL-1$) produced significant cytotoxicity when treated with human mesenchymal stem cells (hMSCs) [67], and at a dose of 50 $\mu ML-1$ MXene, the onset of cell proliferation decreased after 5 days of incubation. At doses of 100 $\mu mL-1$, hMSCs cell proliferation is significantly reduced [67]. Some studies have also suggested that MXene has no toxic effect on cells, and Zhang et al. [68] did not find significant acute cytotoxicity after treating human umbilical vein endothelial cells (HUVECs) with two different concentrations of Ti_3C_2Tx nanosheets (100 and 500 $\mu gmL-1$), respectively. Breast 4T1 cancer cells and glioma U87 cancer cells were treated with PVP-1 concentrations of 0 to 200 μgmL^{-1} with Nb_2CTx nanosheets, and Nb_2CTx nanosheets were found to have no toxic effects [27]. Table 3 summarizes the in vitro biocompatibility tests discussed above.

In vivo

Nasrallah et al. [69] used a zebrafish embryo model to assess in vivo toxicity of Ti_3C_2Tx nanosheets and found that Ti_3C_2Tx nanosheets at doses of 50 μgmL^{-1} did not affect neuronal or muscle activity in zebrafish embryos. Alfussain et al. came to the opposite conclusion [70], using chicken embryos to explore the developmental toxicity of MXene, and experiments at a dose of 30 μg per embryo. Then they found that Ti_3C_2Tx nanosheets had significant toxicity to chicken embryos and observed inhibitory effects on angiogenesis in the choroid, which the analysis suggests may be caused by genes related to down-regulating cell proliferation and angiogenesis. Zhang et al. [71] implanted MXene film into the subcutaneous and calcareous defect sites of rats, and performed micro-CT evaluation and histological analysis on the samples, and the results showed that the MXene film had good bone regeneration and bone induction, and the MXene film neither induced toxic side effects nor caused inflammatory side effects. Bi_2S_3/Ti_3C_2Tx-5 prepared by Li et al. [72] exhibited excellent cytocompatibility and biocompatibility, which can promote the formation of collagen fibers and thus accelerate wound healing. At the same time, its Schottky junction also shows excellent in vivo biosafety. There were also studies that monitored the hematological parameters and biochemical index of Kunning mice after Nb2CTx injection and found no statistical significance, and the results showed that exposure to Nb2CTx nanosheets did not cause significant inflammation [27]. In addition to the above in vivo experiments, there were studies evaluating the effect of MXene on in vivo organs, Sui et al. [73] evaluated the effect of Ti3C2Tx nanosheets on organ function and its distribution in organs, and collected blood, lung, heart and other major organ specimens to determine Ti content after intravenous injection of 20 mg kg^{-1} Ti_3C_2Tx nanosheets in ICR mice, and found that Ti_3C_2Tx nanosheets were mainly distributed in the lungs and liver. The nanosheets accumulated in the liver are gradually excreted through the bile ducts, while the nanosheets in the lungs interfere with respiratory function and lead to respiratory diseases. The above in vivo tests on MXene are summarized in Tables 4 and 5. Current research on MXene's in vivo toxicity is still very limited, and the cytotoxicity and genotoxicity of MXene at the cellular level and the bioaccumulation and biodegradability of MXene within organs both require further research, which is essential

Table 4 In vitro biocompatibility

MXenes	Type of Cells	Dose	Toxicity Effects	Reference
Ti_3C_2Tx	A549, MRC-5, A375, HaCaT cells	0-500 μg mL^{-1}, 24 h	Concentration dependent cytotoxicity. Toxic effects were higher against cancerous cells in comparison to normal ones.	[50]
Ti2NTx	MCF-7, A365, MCF-10 A, HaCaT cells	62.5–500 μg mL^{-1} ,24 h	Higher toxicity to cancer cell lines than normal cell lines	[65]
Ti_3C_2Tx	Human umbilical vein dothelial cells (HUVECs)	100 and 500 μgmL^{-1},48 h	No obvious acute cytotoxicity.	[68]
Ti_3C_2Tx	neural stem cells (NSCs) and NSCs-derived differentiated cells	12.5–100 μg mL^{-1}, 24 h	At 25 μg mL^{-1}, Ti3C2Tx nanosheets caused significant cytotoxicity to NSCs.	[66]
Ti_3C_2Tx	human mesenchymal stem cells (hMSCs)	0-100 μg mL^{-1}, 7 days	> 50 μg mL^{-1}, obvious cytotoxicity was shown	[67]
Nb2CTx	Breast 4T1, glioma U87 cancer cel	0–200 μg mL^{-1}, 24 h	200μgmL^{-1}, no significant cytotoiccity, exposed to NIR, cancer cells were inhibited	[27]

Table 5 In vitro biocompatibility

Mxenes	Type of models	Dose	Toxicity Effects	Reference
Ti_3C_2Tx	Zebrafish embryos	25–200 μg mL^{-1}	At the concentration of 50 μg mL^{-1}, no acutoxicity or neurotoxicity was observed.	[69]
Ti_3C_2Tx	Chicken embryos	30 μg per embryo,5 days incubation	Potential toxicity on the early stage of embryogenesis; down regulation of several controller genes of cell proliferation, survival, cell death and angiogenesis; inhibition of blood vessel development.	[70]
Ti_3C_2Tx	rats	-	No obvious inflammatory and toxic side effects	[71]
Ti_3C_2Tx	rats	-	excellent in vivo biosafety without damaging the main organs	[72]
Ti_3C_2Tx	ICR mice	20 mg kg^{-1}	Ti3C2Tx nanosheets could accumulate in the liver and lungs. Those in the lung might influence respiratory function	[73]
Nb2CTx	Kunming mice	20 mg kg^{-1}	No significant inflammation was caused. No significant histological abnormalities were found.	[27]

for the further development of MXene nano-based medical application products.

To improve the biocompatibility of MXene

In order to be able to better apply MXene nanomaterials, various methods have been used to improve the biocompatibility of MXene, and there have been studies to control toxicity through the interaction between the surface of the MXene phase and collagen [64], and surface modification has improved the biocompatibility of MXene and reduced their oxidative stress, paving the way for future nano applications. Rashid et al. [74] mapped polypropylene glycol (PPG) and polyethylene glycol (PEG) to the surface of Ti3C2Tx nanosheets and evaluated their cytotoxicity for normal (HaCaT and MCF-10 A) and cancerous (MCF-7 and A375) cell lines, a study that provides ideas for nanomaterial applications of wound dressings. Hussein et al. [75] prepared two Ti3C2Tx-based nanocomposites, Namely Au/MXene and Au/Fe3O4/MXene nanocomposites, in the human breast cancer cell line MCF7, while these nanocomposites showed similar photothermal therapeutic efficiencies, hybrid nanocomposites showed lower in vivo toxicity than pure MXene, while in vivo acute toxicity assays using zebrafish embryos indicated the use of Au/MXene and Au/A/. Fe3O4/MXene has reduced embryonic mortality [75], and this study suggests that composites can improve the biocompatibility of MXene. Wojciechowska et al. [76] used the cationic polymer poly L-lysine (PLL) molecule to alter the surface charge of Ti3C2 MXene tablets and tested the cytotoxicity of the resulting Ti3C2/PLL flakes on human skin malignant melanoma cells (A375, ATCC) and human immortal keratinocytes (HaCaT), and the results showed concentrations up to 375 mg L − 1, which did not show cytotoxicity. Similarly, Wang et al. [77] coated silkenin on an MXene film and performed

cytotoxicity tests using human skin fibroblast HSAS1 cells, the silken protein-coated MXene showed about 99% cell viability after 6 days of incubation, and fluorescent image analysis showed no significant change in viability even when exposed to the silkin-coated MXene membrane HSAS1 cells, suggesting that the silkin-coated MXene film had better biocompatibility. As mentioned above, there have been considerable studies on surface modification of MXenes, and relatively satisfactory results have been achieved, but there is still a lack of in vivo tests to prove short-term and long-term safety in vivo.

The application of MXene in wound healing

At present, many scholars have developed new composite materials for the production of wound dressings, which are based on MXene nanomaterials and make full use of their excellent properties as mentioned above, and play a role in sterilization, drug-carrying sustained release, active regulation of cytokines and other functions in the skin wounds, which greatly enriches the ideas and means of treating chronic wounds. We summarize the currently retrieved MXene composites for promoting skin healing, and divide them into 4 parts according to the mechanism of action (Fig. 5).

Improving the tissue repair properties

Li et al. [78] prepared anisotropic MXene@PVA hydrogels by directional freezing-assisted salting out method. The hydrogel was characterized by its excellent mechanical properties (stress up to 0.5 MPa, strain up to 800%), excellent photothermal properties (localized hyperthermia can be applied to the infected site using NIR laser-808 nm), Broad-spectrum antibacterial activity (inhibition rates of Escherichia coli and Staphylococcus aureus were 98.3% and 95.5%, respectively) and promoted the proliferation of NIH-3T3 cells. In a mouse wound model, the hydrogel was found to effectively inhibit wound infection and promote Skin wound healing (98% wound closure rate). The results show that MXene@PVA hydrogel has high toughness and anisotropy, and is an excellent candidate material for wound dressings. In addition to antibacterial and pro-proliferation properties, hemostasis is also an important property for novel wound dressings. Li et al. [79] prepared a composite

Fig. 5 The application of mxene

sponge by incorporating MXene-based nanomaterials into a chitin sponge (CH) network to achieve. The purpose of hemostasis and promotion of wound healing. After the addition of MXene-based nanomaterials, the hemostatic effect of the composite sponge was significantly enhanced due to the improvement of hemophilicity and the acceleration of blood coagulation kinetics. Moreover, the composite sponge showed excellent antibacterial activity through the synergistic effect between trapping and photothermal effects. In vivo experiments demonstrated that the wound closure rate was 84% on day 9 [79]. In addition to composite hydrogels, composite sponges, etc., composite scaffold systems prepared from various materials have also been used in skin dressing research. Zhou et al. [80] combined polyglycerol-ethylene amine, Ti3C2Tx MXene@polydopamine (MXene@ PDA) nanosheets were reacted with oxidized hyaluronic acid (HCHO) to prepare HPEM scaffolds. Studies have confirmed that the scaffold has excellent rheological properties, self-healing, electrical conductivity, and tissue adhesion properties. Meanwhile, the HPEM scaffold has high antibacterial activity against Escherichia coli, Staphylococcus aureus, and MRSA, and can also stimulate cell proliferation, upregulate α muscle Actin, COL III and VEGF gene expression. Using a full-thickness MRSA-infected wound model, HPEM scaffolds were found to promote early angiogenesis in infected wounds and significantly enhance wound healing in MRSA-infected wounds [80, 81].They prepared composites by combining Ti_3C_2Tx MXene with antioxidant CeO_2 and incorporated them into polyethyleneimine-grafted polyethylene ions F127 (F127-PEI) and the dynamics of oxidized sodium alginate (OSA). Formation of FOM scaffolds in Schiff-based chemically cross-linked hydrogels. This FOM stent has various functional properties, such as injectable, antibacterial, electrical conductivity, and rapid hemostasis. In vitro and in vivo experiments confirmed that the FOM scaffold could promote fibroblast migration and proliferation, granulation tissue formation, collagen deposition, and re-epithelialization to accelerate MDR-infected wound healing through electrical stimulation [81]. By combining MXene nanomaterials with various traditional materials, new composite materials such as hydrogels, composite sponges, and composite scaffolds are prepared for the preparation of wound dressings. These dressings not only exhibit the inherent properties of MXene, but also can exert the functional properties of other traditional excipients, synergistically Complementary increases the tissue repair ability of the dressing to achieve the purpose of promoting wound healing, providing a new means for wound treatment and a new idea for the research and development of new wound dressings.

Mxene marix material-assisted photothermal therapy

Near-infrared (NIR) laser-based photothermal therapy (PTT) uses a photothermal agent as an internal energy absorber to locally convert NIR light energy into heat energy to generate high heat to cause necrosis or apoptosis of target cells. More and more scholars have discovered that photothermal therapy can be used to promote skin wound healing in addition to cancer treatment Zhu [82] et al. used the idea of photothermal therapy (PTT) to construct Ag/Ti_3C_2Tx composites with MXene nanomaterials with excellent photothermal properties together with Ag. The antibacterial effects of Staphylococcus aureus and Gram-negative Escherichia coli were significantly enhanced compared with the application of Ag or Ti_3C_2Tx alone, which indicated that the antibacterial properties of Ag and Ti_3C_2Tx photothermal sterilization had a synergistic effect, and the cytotoxicity results showed that Ag/Ti_3C_2Tx had better Based on their biocompatibility, they were embedded in hydrogels for use as wound dressings and found that they exhibited excellent bacterial inhibition and wound healing-promoting properties under near-infrared light irradiation. Zhang et al. [83] prepared MXene/zeolite imidazole framework-8 (ZIF-8)/polylactic acid (PLA) composite membrane (MZ-8/PLA) by electrospinning process, which was irradiated by 808 nm laser. It exhibits effective PTT and photodynamic therapy (PDT) properties. In vitro experiments show that the antibacterial rates of MZ-8/PLA against Escherichia coli and methicillin-resistant Staphylococcus aureus are as high as 99.9% and 99.8%, respectively. In vivo experiments confirmed that MZ-8 /PLA can accelerate the healing of bacterially infected wounds without developing drug resistance.

The antimicrobial effect of photosensitive biomedical materials produces free radical oxygen (ROS) under light in addition to converting NIR to local thermal energy [84]. Li et al. [85] constructed the interface Schottky junction of Bi_2S_3/Ti_3C_2Tx, envisioning enhanced photocatalytic performance by accelerating photo-induced charge transfer to improve ROS yields for antimicrobial purposes, in vitro experiments by spread plate, live/dead fluorescence staining, and SEM antibacterial images. Other techniques have found that Bi_2S_3/Ti_3C_2Tx-5 has obvious antibacterial effects on Staphylococcus aureus and Escherichia coli, and the synergistic effect of ROS and photothermal therapy has better antibacterial properties compared with the use of ROS or photothermal therapy alone, and it was found that Bi_2S_3/Ti_3C_2Tx Schottky knot significantly promoted wound healing under 808 nm near-infrared irradiation. Similarly, Zhou et al. [86] designed and developed PLGA scaffolds with MXene as a matrix material, and Zhou et al. believe that PLGA membranes can exert a photothermal effect to

generate reactive oxygen species under near-infrared light and gradually degrade to lactate, while the Lox component in the membrane can consume lactate to produce hydrogen peroxide (H_2O_2) and catalyze the resulting H_2O_2 into hydroxyl radicals through a Fenton-like reaction to achieve rapid co-sterilization. In vivo assays have shown that nanocatalytic membranes will delay the regeneration of chronic wound wounds that delay healing by antibacterial, hemostatic, local collagen deposition in wounds, and angiogenesis [86]. By producing exogenous reactive oxygen species (ROS) is a good new antibacterial concept, but due to the presence of endogenous antioxidant glutathione (GSH) in bacteria, exogenous reactive oxygen species (ROS) produced solely by light therapy may be difficult to achieve the desired antibacterial effect, Yang et al. [87] proposed a solution by preparing an antibacterial nano platform of Ti_3C_2/MoS_2 bioisomer (HJ), which has photothermal, photodynamic, peroxidase-like and glutathione-like properties. Under near-infrared (NIR) laser irradiation, biological HJ not only produces local heating but also increases extracellular ROS levels, resulting in bacterial inactivation, while Mo^{+4} ions can invade the bacterial membrane to increase intracellular ROS content and consume intracellular GSH, and the internal and external synergistic antibacterial effects are produced. In vitro tests confirmed that biological HJ exhibited good cytocompatibility and promoted cell migration in vitro after loading FGF21. In vivo evaluation using a mouse infected wound model demonstrated that the antimicrobial platform had excellent antibacterial infection and accelerated wound healing. The above research results fully apply the photothermal properties of MXene nanomaterials, and the photothermal agent used as a composite material produces antibacterial properties and synergizes with the antibacterial properties of itself or other materials, making MXene one of the best alternative antibiotics to solve drug resistance and infected wounds.

MXene matrix material-assisted electrical stimulation therapy

When the epithelium is damaged, it itself generates an endogenous direct current electric field (DCEF) and a transepithelial potential (TEP) difference that drives the current out of the injured area and persists locally until the healing process is complete. Many epithelial cells, including human keratinocytes, are able to detect this electric field and make directional migration [88]. At the same time, the physiological DC electric field generated by epithelial damage can actively regulate cell behavior, enhance angiogenesis [88], block edema formation, down-regulate inflammatory factors, promote granulation tissue formation, promote collagen synthesis [89–92], and induce skin wounds. Re-epithelialization [93–95]. When the electric field was removed, wound healing slowed by 25% [88], suggesting that electrical stimulation can effectively promote skin wound healing, however, most wound dressings are not electrically active, and therefore do not have any effect on the wound site during the healing process. Responding to physiological electrical signals or external ES, which has become a major criticism of current wound dressings. To provide a physical platform for cell growth and tissue repair while also allowing localized current delivery at the wound site, Lin et al. [96] prepared bacterial cellulose/MXene (rBC/MXene) hydrogels by chemical and physical dual crosslinking method The hydrogel system can accelerate skin healing by simulating the wound healing mechanism in response to exogenous electrical stimulation (ES) according to the action of the endogenous electric field. Experiments have demonstrated that in the presence of external ES, the hydrogel and ES can synergistically enhance the proliferative activity of NIH3T3 cells in vitro and actively accelerate the wound healing process in vivo (such as reduction of wound area, enhancement of collagen synthesis and angiogenesis), It also promotes granulation tissue formation, re-epithelialization, and growth factor (including VEGF, EGF, and TGF-β) release compared with non-ES controls [96]. Overall, the biodegradable electroactive rBC/MXene hydrogel developed in this study is a promising candidate as a wound dressing for cutaneous wound healing, and this study provides evidence for promoting wound repair. An effective synergistic therapeutic strategy, which is of great significance for the development of MXene-assisted electrical stimulation therapy for wound treatment.

MXene materials as drug carriers for promoting skin damage repair

The use of chemical or biological agents such as drug intervention is one of the most popular methods to promote wound healing, and drug delivery systems based on different morphological designs have been proposed to prolong the drug release time and reduce the potential toxicity of drugs [97, 98]. Stimuli-responsive hydrogel systems have emerged as promising drug delivery vehicles for wound management. Yang et al. [99] developed a hydrogel system composed of MXene-encapsulated magnetic colloids and poly(N-isopropylacrylamide)-alginate double-net hydrogels to deliver photosensitizing and magnetically responsive drugs to deep chronic wounds, the results show that the hydrogel system constructed in this study has controllable drug delivery ability, which can reduce the toxic and side effects of drugs and promote wound healing. role [99]. Hao et al. [100] developed a K-M/PNIPAm hydrogel dressing based on

conductive MXene nanosheets and temperature-sensitive PNIPAm polymer, and the novel hydrogel dressing was found to be strain-sensitive as well as to NIR phase transition and volume change The responsiveness of the hydrogel when used as a strain flexible sensor shows high sensitivity (gauge factor-GF is 4.491), wide strain range (about 250%), fast response speed (close to 160 ms), and good cycling stability properties (3000 s at 20% strain). Therefore, this K-M/PNIPAm hydrogel can be used as an efficient NIR light-controlled drug release carrier for on-demand drug release in deep wounds [100]. In addition to hydrogel systems, microneedle systems have also received great research interest in constructing drug delivery systems because they can penetrate the skin non-invasively and painlessly [101, 102]. Based on the above problems, Sun et al. [103] proposed 3 -(Acrylamido)phenylboronic acid-(PBA-) integrated polyethylene glycol diacrylate (PEGDA) hydrogel as host material to prepare microneedle patch, the authors believe that the derived PBA patch can not only provide exogenous adenosine It also has the ability to chelate endogenous adenosine for damage repair, and MXene can rapidly convert light into heat under near-infrared (NIR) irradiation to accelerate the release of loaded adenosine. In vitro experiments showed that MXene-integrated PBA hydrogel. The hydrogel had no negative effect on cell growth, while the adenosine-encapsulated MXene-integrated microneedle patch enhanced angiogenesis. Animal model results demonstrated that the functional microneedle patch could effectively promote angiogenesis and accelerate the wound healing process. The microneedle patch system can actively deliver and use natural molecules, which greatly enriches the variety of this type of research. Inspired by the flat and inclined structure of shark teeth, Guo et al. [104] fabricated biomimetic microneedle patches by replicating laser-engraved negative molds and using origami, which enabled the microneedle patches to have stable adhesion in tissues Adhesion, using porous ordered structures and temperature-responsive hydrogels to build controllable drug release systems on microneedle patches. Experiments in diabetic rats demonstrated that drug-loaded biomimetic microneedle patches can promote full-thickness skin wound recovery [104]. The electrospinning process has been widely used in the biomedical field. Electrospinning nanofibrous membranes have a three-dimensional network structure, which is widely studied as a promising wound healing method because it can maintain the moisture absorption balance of the wound site and promote wound healing. dressings [105]. Xu et al. [106] mixed and electrospun amoxicillin (AMX), MXene, and polyvinyl alcohol (PVA) into an antibacterial nanofibrous membrane (MXene-AMX-PVA nanofibrous membrane) for making wound dressings. In the composite nanofibrous membrane, the PVA matrix can control the release of AMX to combat bacterial infection, while the MXene can convert the near-infrared laser light into heat, resulting in localized hyperthermia to promote AMX release. At the same time, localized hyperthermia can also synergistically lead to bacterial inactivation. The antibacterial activity and wound healing ability of the composite nanofiber membrane were systematically verified in a mouse skin defect model infected

Table 6 The application of MXene in wound healing

MXenes	Scaffold type	Result	Reference
Ti_3C_2Tx	composite hydrogels	High toughness, anisotropy, antibacterial activity and cell proliferation	[78]
Ti_3C_2Tx	composite sponge	Enhanced hemostatic effect	[79]
Ti_3C_2Tx	HPEM scaffolds	Excellent rheological properties, self-healing properties, electrical conductivity and tissue adhesion properties	[80]
Ti_3C_2Tx	FOM scaffolds	Injectable, antibacterial, conductive and quick hemostatic	[81]
Ti_3C_2Tx	Ag/ Ti_3C_2Tx composites	Bacteria inhibit and promote wound healing	[82]
Ti_3C_2Tx	MZ-8/PLA composite membrane	Accelerates bacterial wound healing without developing drug resistance	[83]
Ti_3C_2Tx	Interface Schottky junction	Antibacterial and promote wound healing	[85]
Ti_3C_2Tx	PLGA membranes	Antibacterial, hemostatic, promote wound local collagen deposition and promote angiogenesis	[86]
Ti_3C_2	Ti_3C_2/MoS_2 bioheterojunction	Photothermal, photodynamic, peroxidase - like and glutathione oxidase - like properties	[87]
Ti_3C_2Tx	rBC/MXene hydrogels	In response to exogenous electrical stimulation	[96]
Ti_3C_2Tx	Double-net hydrogels	Controlled drug delivery capability	[99]
Ti_3C_2Tx	K-M/PNIPAm hydrogel dressing	Photocontrolled drug release ability	[100]
Ti_3C_2Tx	PEGDA microneedle patch	Promote angiogenesis, accelerate wound healing and active delivery	[103]
Ti_3C_2Tx	Biomimetic microneedle patches	Controlled drug release	[104]
Ti_3C_2Tx	MXene-AMX-PVA nanofibrous membrane	Physical barrier, high antibacterial	[106]

with Staphylococcus aureus. The film not only functions as a co-loaded physical barrier for AMX and MXene, but also exhibits high antibacterial and accelerated wound healing abilities [106]. The drug-loading system based on MXene nanomaterials can solve the difficult problem of local drug delivery in deep tissue, and propose a new solution for tissue repair. The application of MXene in wound healing are summarized in Table 6.

Discussion

With adjustable surface termination, excellent performance, satisfactory properties, and suitable for a variety of biomedical applications, MXene has achieved the control of toxic side effects of the synthesis process and the properties of synthetic products by selecting the preparation method. Various composites developed based on the various properties of MXene have achieved satisfactory results in wound antibacterial and repair, showing that they are in the initial stage of development in the field of promoting skin repair and have great development prospects. At the same time, we should not only invest in developing MXene materials to promote skin healing, but also focus on finding toxicity testing solutions that meet the requirements. At present, although some scholars have conducted studies on the cytotoxicity and compatibility of related materials, these studies are based on cell experiments or short-term hematological assays, the long-term biosecurity of MXene has not been systematically evaluated, and the existing in vivo compatibility studies are carried out in low-level animal models (such as mice and zebrafish) and do not involve higher-order mammals such as monkeys or dogs, so we need to conduct more systematic MXene long-term toxicity experiments and in vivo studies of higher-level animals. This is crucial for evaluating the safety of the application of MXene materials in vivo. All in all, there are bright prospects for the study of MXene-based wound dressings and their application to clinical treatment, but we still have a long way to go.

Acknowledgements
Not applicable.

Authors' contributions
Chengzhi Liang.Jing He and Yuan Cao wrote the main manuscript text and Guoming Liu. Chengdong Zhang. Zhiping Qi prepared figures and tables. yanling Hu and Chuan Fu check the manuscriot. All authors reviewed the manuscript. The author(s) read and approved the final manuscript.

Funding
This work was supported by the National Natural Science Foundation of China (32000828) and the Natural Science Foundation of Jilin Provincial Science and Technology Department (20200201454JC).

Availability of dataand materials
Not applicable.

Declarations

Competing interests
The authors declare no competing interests.

Ethics approval and consent to participate
Not applicable.

Consent for publication
Not applicable.

Received: 8 August 2022 Accepted: 15 May 2023
Published online: 08 June 2023

References

1. Gurtner GC, Werner S, Barrandon Y, Longaker MT. Wound repair and regeneration. Nature. 2008;453(7193):314–21.
2. Abazari M, et al. A systematic review on classification, identification, and Healing process of burn Wound Healing. Int J Low Extrem Wounds. 2022;21(1):18–30.
3. Yang Y, et al. A quaternized chitin derivatives, egg white protein and montmorillonite composite sponge with antibacterial and hemostatic effect for promoting wound healing. Compos B Eng. 2022. p. 234.
4. Werner S, Krieg T, Smola H. Keratinocyte-fibroblast interactions in wound healing. J Invest Dermatol. 2007;127(5):998–1008.
5. Lovvorn HN 3rd, Cheung DT, Nimni ME, Perelman N, Estes JM, Adzick NS. Relative distribution and crosslinking of collagen distinguish fetal from adult sheep wound repair. J Pediatr Surg. 1999;34(1):218–23.
6. Fu C, Qi Z, Zhao C, Kong W, Li H, Guo W, et al. Enhanced wound repair ability of arginine-chitosan nanocomposite membrane through the antimicrobial peptides-loaded polydopamine-modified graphene oxide. J Biol Eng. 2021;15(1):17.
7. Gehring J, Trepka B, Klinkenberg N, Bronner H, Schleheck D, Polarz S. Sunlight-triggered nanoparticle synergy: teamwork of reactive oxygen species and nitric oxide released from Mesoporous Organosilica with Advanced Antibacterial Activity. J Am Chem Soc. 2016;138(9):3076–84.
8. Roope LSJ, Smith RD, Pouwels KB, Buchanan J, Abel L, Eibich P, et al. The challenge of antimicrobial resistance: what economics can contribute. Volume 364. New York, NY: Science; 2019. 6435.
9. Murphy PS, Evans GR. Advances in wound healing: a review of current wound healing products. Plast Surg Int. 2012;2012:190436.
10. Alven S, Aderibigbe BA. Hyaluronic acid-based scaffolds as potential bioactive wound dressings. Polymers. 2021;13(13):2102.
11. Walker BW, Lara RP, Mogadam E, Yu CH, Kimball W, Annabi N. Rational design of Microfabricated Electroconductive Hydrogels for Biomedical Applications. Prog Polym Sci. 2019;92:135–57.
12. Vijayakumar V, Samal SK, Mohanty S, Nayak SK. Recent advancements in biopolymer and metal nanoparticle-based materials in diabetic wound healing management. Int J Biol Macromol. 2019;122:137–48.
13. Hamdan S, Pastar I, Drakulich S, Dikici E, Tomic-Canic M, Deo S, et al. Nanotechnology-driven therapeutic interventions in Wound Healing: potential uses and applications. ACS Cent Sci. 2017;3(3):163–75.
14. Arafa MG, El-Kased RF, Elmazar MM. Thermoresponsive gels containing gold nanoparticles as smart antibacterial and wound healing agents. Sci Rep. 2018;8(1):13674.
15. Mârza SM, Magyari K, Bogdan S, Moldovan M, Peştean C, Nagy A, et al. Skin wound regeneration with bioactive glass-gold nanoparticles ointment. Biomed Mater. 2019;14(2):025011.
16. Kumar PT, Lakshmanan VK, Anilkumar TV, Ramya C, Reshmi P, Unnikrishnan AG, et al. Flexible and microporous chitosan hydrogel/nano ZnO composite bandages for wound dressing: in vitro and in vivo evaluation. ACS Appl Mater Interfaces. 2012;4(5):2618–29.
17. Tadej M. The use of Flivasorb in highly exuding wounds. Br J Nurs. 2009;18(15):38. s40-2.
18. Dodane V, Vilivalam VD. Pharmaceutical applications of chitosan. Pharm Sci Technol Today. 1998;1(6):246–53.

19. Fu L, Zhang J, Yang G. Present status and applications of bacterial cellulose-based materials for skin tissue repair. Carbohydr Polym. 2013;92(2):1432–42.
20. Ye H, Cheng J, Yu K. In situ reduction of silver nanoparticles by gelatin to obtain porous silver nanoparticle/chitosan composites with enhanced antimicrobial and wound-healing activity. Int J Biol Macromol. 2019;121:633–42.
21. Anasori B, Lukatskaya MR, Gogotsi Y. 2D metal carbides and nitrides (MXenes) for energy storage. Nat Rev Mater. 2017;2(2):17.
22. Naguib M, Gogotsi Y. Synthesis of Two-Dimensional materials by selective extraction. Acc Chem Res. 2015;48(1):128–35.
23. Huang K, Li Z, Lin J, Han G, Huang P. Two-dimensional transition metal carbides and nitrides (MXenes) for biomedical applications. Chem Soc Rev. 2018;47(14):5109–24.
24. Sang X, Xie Y, Lin MW, Alhabeb M, Van Aken KL, Gogotsi Y, et al. Atomic defects in monolayer Titanium Carbide (Ti(3)C(2)T(x)) MXene. ACS Nano. 2016;10(10):9193–200.
25. Dillon AD, Ghidiu MJ, Krick AL, Griggs J, May SJ, Gogotsi Y, et al. Highly conductive optical quality solution-processed Films of 2D Titanium Carbide. Adv Funct Mater. 2016;26(23):4162–8.
26. Chen K, Qiu N, Deng Q, Kang MH, Yang H, Baek JU, et al. Cytocompatibility of Ti(3)AlC(2), Ti(3)SiC(2), and Ti(2)AlN: in Vitro tests and first-principles calculations. ACS biomaterials science & engineering. 2017;3(10):2293–301.
27. Lin H, Gao S, Dai C, Chen Y, Shi JA, Two-Dimensional. Biodegradable Niobium Carbide (MXene) for Photothermal Tumor Eradication in NIR-I and NIR-II Biowindows. J Am Chem Soc. 2017;139(45):16235–47.
28. Zamhuri A, Lim GP, Ma NL, Tee KS, Soon CF. MXene in the lens of biomedical engineering: synthesis, applications and future outlook. Biomed Eng Online. 2021;20(1):33.
29. Huang K, Li ZJ, Lin J, Han G, Huang P. Two-dimensional transition metal carbides and nitrides (MXenes) for biomedical applications. Chem Soc Rev. 2018;47(14):5109–24.
30. Naguib M, Kurtoglu M, Presser V, Lu J, Niu JJ, Heon M, et al. Two-dimensional nanocrystals produced by exfoliation of Ti3AlC2. Adv Mater. 2011;23(37):4248–53.
31. Alhabeb M, Maleski K, Anasori B, Lelyukh P, Clark L, Sin S, et al. Guidelines for synthesis and Processing of two-dimensional Titanium Carbide (Ti3C2TX MXene). Chem Mat. 2017;29(18):7633–44.
32. Zhou AG, Barsoum MW. Kinking nonlinear elastic deformation of Ti3AlC2, Ti2AlC, Ti3Al(C-0.5,N-0.5)(2) and Ti2Al(C-0.5,N-0.5). J Alloy Compd. 2010;498(1):62–70.
33. Tzenov NV, Barsoum MW. Synthesis and characterization of Ti3AlC2 (vol 83, pg 825, 2000). J Am Ceram Soc. 2000;83(6):1551.
34. Pang SY, Wong YT, Yuan S, Liu Y, Tsang MK, Yang Z, et al. Universal Strategy for HF-Free Facile and Rapid Synthesis of two-dimensional MXenes as multifunctional energy materials. J Am Chem Soc. 2019;141(24):9610–6.
35. Halim J, Lukatskaya MR, Cook KM, Lu J, Smith CR, Näslund LA, et al. Transparent conductive two-dimensional Titanium Carbide Epitaxial Thin Films. Chem materials: publication Am Chem Soc. 2014;26(7):2374–81.
36. Ahmad S, Ashraf I, Mansoor MA, Rizwan S, Iqbal M. An overview of recent advances in the synthesis and applications of the Transition Metal Carbide Nanomaterials. Nanomaterials (Basel Switzerland). 2021;11(3):776.
37. Zhou J, Zha X, Chen FY, Ye Q, Eklund P, Du S, et al. A Two-Dimensional Zirconium Carbide by Selective Etching of Al3C3 from Nanolaminated Zr3Al3C5. Angewandte Chemie (International ed in English). 2016;55(16):5008–13.
38. Li Z, Yu L, Milligan C, Ma T, Zhou L, Cui Y, et al. Two-dimensional transition metal carbides as supports for tuning the chemistry of catalytic nanoparticles. Nat Commun. 2018;9(1):5258.
39. Xu C, Wang L, Liu Z, Chen L, Guo J, Kang N, et al. Large-area high-quality 2D ultrathin Mo2C superconducting crystals. Nat Mater. 2015;14(11):1135–41.
40. Xiao X, Yu H, Jin H, Wu M, Fang Y, Sun J, et al. Salt-Templated synthesis of 2D metallic MoN and other Nitrides. ACS Nano. 2017;11(2):2180–6.
41. Yang BW, Chen Y, Shi JL. Material Chemistry of Two-Dimensional Inorganic Nanosheets in Cancer Theranostics. Chem. 2018;4(6):1284–313.
42. Zhu J, Ha EN, Zhao GL, Zhou Y, Huang DS, Yue GZ, et al. Recent advance in MXenes: a promising 2D material for catalysis, sensor and chemical adsorption. Coord Chem Rev. 2017;352:306–27.
43. Zhang YJ, Wang L, Zhang NN, Zhou ZJ. Adsorptive environmental applications of MXene nanomaterials: a review. RSC Adv. 2018;8(36):19895–905.
44. Rasool K, Helal M, Ali A, Ren CE, Gogotsi Y, Mahmoud KA. Antibacterial Activity of Ti_3C_2Tx MXene. ACS Nano. 2016;10(3):3674–84.
45. Shamsabadi AA, Gh MS, Anasori B, Soroush M. Antimicrobial Mode-of-action of Colloidal Ti3C2TX MXene Nanosheets. ACS Sustain Chem Eng. 2018;6(12):16586–96.
46. Li RY, Zhang LB, Shi L, Wang P. MXene Ti3C2: an effective 2D light-to-heat Conversion Material. ACS Nano. 2017;11(4):3752–9.
47. Lin H, Wang XG, Yu LD, Chen Y, Shi JL. Two-dimensional ultrathin MXene ceramic nanosheets for Photothermal Conversion. Nano Lett. 2017;17(1):384–91.
48. Zhao MQ, Xie XQ, Ren CE, Makaryan T, Anasori B, Wang GX, et al. Hollow MXene spheres and 3D macroporous MXene frameworks for Na-Ion storage. Adv Mater. 2017;29(37):7.
49. Kim SJ, Koh HJ, Ren CE, Kwon O, Maleski K, Cho SY, et al. Metallic Ti3C2TX MXene Gas Sensors with Ultrahigh Signal-to-noise ratio. ACS Nano. 2018;12(2):986–93.
50. Jastrzębska AM, Szuplewska A, Wojciechowski T, Chudy M, Ziemkowska W, Chlubny L, et al. In vitro studies on cytotoxicity of delaminated Ti(3)C(2) MXene. J Hazard Mater. 2017;339:1–8.
51. Lim GP, Soon CF, Morsin M, Ahmad MK, Nayan N, Tee KS. Synthesis, characterization and antifungal property of Ti3C2Tx MXene nanosheets. Ceram Int. 2020;46(12):20306–12.
52. Lin H, Wang Y, Gao S, Chen Y, Shi J. Theranostic 2D Tantalum Carbide (MXene). Advanced materials (Deerfield Beach, Fla). 2018;30(4):11.
53. Hu JP, Xu B, Ouyang CY, Zhang Y, Yang SYA. Investigations on Nb2C monolayer as promising anode material for Li or non-li ion batteries from first-principles calculations. RSC Adv. 2016;6(33):27467–74.
54. Zhao SJ, Kang W, Xue JM. MXene nanoribbons. J Mater Chem C. 2015;3(4):879–88.
55. Naguib M, Kurtoglu M, Presser V, Lu J, Niu J, Heon M, et al. Two-dimensional nanocrystals produced by exfoliation of Ti3 AlC2. Advanced materials (Deerfield Beach. Fla). 2011;23(37):4248–53.
56. Lai S, Jeon J, Jang SK, Xu J, Choi YJ, Park JH, et al. Surface group modification and carrier transport properties of layered transition metal carbides (Ti2CTx, T: -OH, -F and -O). Nanoscale. 2015;7(46):19390–6.
57. Zazoum B, Bachri A, Nayfeh J. Functional 2D MXene inks for Wearable Electronics. Mater (Basel Switzerland). 2021;14(21):6603.
58. Zhang YZ, Lee KH, Anjum DH, Sougrat R, Jiang Q, Kim H, et al. MXenes stretch hydrogel sensor performance to new limits. Sci Adv. 2018;4(6):7.
59. He SS, Sun X, Zhang H, Yuan CD, Wei YP, Li JJ. Preparation strategies and applications of MXene-Polymer Composites: a review. Macromol Rapid Commun. 2021;42(19):23.
60. Damiri F, Rahman MH, Zehravi M, Awaji AA, Nasrullah MZ, Gad HA et al. MXene (Ti3C2Tx)-Embedded nanocomposite hydrogels for Biomedical Applications: a review. Mater (Basel Switzerland). 2022;15(5):1666.
61. Ahmad S, Ashraf I, Mansoor MA, Rizwan S, Iqbal M. An overview of recent advances in the synthesis and applications of the Transition Metal Carbide Nanomaterials. Nanomaterials. 2021;11(3):34.
62. Li KK, Jiao TF, Xing RR, Zou GD, Zhou JX, Zhang LX, et al. Fabrication of tunable hierarchical MXene@AuNPs nanocomposites constructed by self-reduction reactions with enhanced catalytic performances. Sci China-Mater. 2018;61(5):728–36.
63. Chimene D, Alge DL, Gaharwar AK. Two-dimensional nanomaterials for Biomedical Applications: emerging Trends and Future prospects. Adv Mater. 2015;27(45):7261–84.
64. Rozmyslowska-Wojciechowska A, Szuplewska A, Wojciechowski T, Pozniak S, Mitrzak J, Chudy M, et al. A simple, low-cost and green method for controlling the cytotoxicity of MXenes. Mater Sci Eng C-Mater Biol Appl. 2020;111:8.
65. Szuplewska A, Rozmysłowska-Wojciechowska A, Poźniak S, Wojciechowski T, Birowska M, Popielski M, et al. Multilayered stable 2D nano-sheets of Ti(2)NT(x) MXene: synthesis, characterization, and anticancer activity. J Nanobiotechnol. 2019;17(1):114.

66. Wu W, Ge H, Zhang L, Lei X, Yang Y, Fu Y, et al. Evaluating the cytotoxicity of Ti(3)C(2) MXene to neural stem cells. Chem Res Toxicol. 2020;33(12):2953–62.
67. Jang JH, Lee EJ. Influence of MXene particles with a stacked-lamellar structure on osteogenic differentiation of human mesenchymal stem cells. Mater (Basel Switzerland). 2021;14(16):4453.
68. Zhang DK, Zheng W, Li X, Li A, Ye N, Zhang L, et al. Investigating the effect of Ti3C2 (MXene) nanosheet on human umbilical vein endothelial cells via a combined untargeted and targeted metabolomics approach. Carbon. 2021;178:810–21.
69. Nasrallah GK, Al-Asmakh M, Rasool K, Mahmoud KA. Ecotoxicological assessment of Ti3C2Tx (MXene) using a zebrafish embryo model. Environ Sci-Nano. 2018;5(4):1002–11.
70. Alhussain H, Augustine R, Hussein EA, Gupta I, Hasan A, Al Moustafa AE, et al. MXene Nanosheets May induce toxic effect on the early stage of Embryogenesis. J Biomed Nanotechnol. 2020;16(3):364–72.
71. Zhang JB, Fu Y, Mo AC. Multilayered Titanium Carbide MXene Film for guided bone regeneration. Int J Nanomed. 2019;14:10091–102.
72. Li J, Li Z, Liu X, Li C, Zheng Y, Yeung KWK, et al. Interfacial engineering of Bi(2)S(3)/Ti(3)C(2)T(x) MXene based on work function for rapid photo-excited bacteria-killing. Nat Commun. 2021;12(1):1224.
73. Sui B, Liu X, Sun J. Biodistribution, inter-/intra-cellular localization and respiratory dysfunction induced by Ti(3)C(2) nanosheets: involvement of surfactant protein down-regulation in alveolar epithelial cells. J Hazard Mater. 2021;402:123562.
74. Rashid B, Anwar A, Shahabuddin S, Mohan G, Saidur R, Aslfattahi N, et al. A comparative study of cytotoxicity of PPG and PEG Surface-Modified 2-D Ti3C2 MXene Flakes on Human Cancer cells and their Photothermal response. Materials. 2021;14(16):14.
75. Hussein EA, Zagho MM, Rizeq BR, Younes NN, Pintus G, Mahmoud KA, et al. Plasmonic MXene-based nanocomposites exhibiting photothermal therapeutic effects with lower acute toxicity than pure MXene. Int J Nanomed. 2019;14:4529–39.
76. Rozmyslowska-Wojciechowska A, Mitrzak J, Szuplewska A, Chudy M, Wozniak J, Petrus M, et al. Engineering of 2D Ti3C2 MXene Surface Charge and its influence on Biological Properties. Materials. 2020;13(10):18.
77. Wang DY, Wang LL, Lou Z, Zheng YQ, Wang K, Zhao LJ, et al. Biomimetic, biocompatible and robust silk Fibroin-MXene film with stable 3D cross-link structure for flexible pressure sensors. Nano Energy. 2020;78:8.
78. Li Y, Han MM, Cai Y, Jiang B, Zhang YX, Yuan BA, et al. Muscle-inspired MXene/PVA hydrogel with high toughness and photothermal therapy for promoting bacteria-infected wound healing. Biomater Sci. 2022;10(4):1068–82.
79. Li S, Gu B, Li X, Tang S, Zheng L, Ruiz-Hitzky E et al. MXene-Enhanced chitin composite sponges with antibacterial and hemostatic activity for Wound Healing. Adv Healthc Mater. 2022;11(12):e2102367.
80. Zhou L, Zheng H, Liu ZX, Wang SQ, Liu Z, Chen F, et al. Conductive antibacterial hemostatic multifunctional scaffolds based on Ti3C2Tx MXene nanosheets for promoting Multidrug-Resistant Bacteria-infected Wound Healing. ACS Nano. 2021;15(2):2468–80.
81. Zheng H, Wang SQ, Cheng F, He XW, Liu ZX, Wang WY, et al. Bioactive anti-inflammatory, antibacterial, conductive multifunctional scaffold based on MXene@CeO2 nanocomposites for infection-impaired skin multimodal therapy. Chem Eng J. 2021;424:12.
82. Zhu XQ, Zhu YN, Jia K, Abraha BS, Li Y, Peng WC, et al. A near-infrared light-mediated antimicrobial based on Ag/Ti(3)C(2)T(x) for effective synergetic antibacterial applications. Nanoscale. 2020;12(37):19129–41.
83. Zhang SQ, Ye JW, Liu X, Wang Y, Li C, Fang JT, et al. Titanium carbide/zeolite imidazole framework-8/polylactic acid electrospun membrane for near-infrared regulated photothermal/ photodynamic therapy of drug-resistant bacterial infections. J Colloid Interface Sci. 2021;599:390–403.
84. Li M, Li L, Su K, Liu X, Zhang T, Liang Y, et al. Highly Effective and Noninvasive Near-Infrared Eradication of a Staphylococcus aureus Biofilm on Implants by a Photoresponsive Coating within 20 Min. Advanced science (Weinheim, Baden-Wurttemberg, Germany). 2019;6(17):1900599.
85. Li JF, Li ZY, Liu XM, Li CY, Zheng YF, Yeung KWK, et al. Interfacial engineering of Bi2S3/Ti3C2Tx MXene based on work function for rapid photo-excited bacteria-killing. Nat Commun. 2021;12(1):10.
86. Zhou X, Wang ZY, Chan YK, Yang YM, Jiao Z, Li LM, et al. Infection Micromilieu-Activated nanocatalytic membrane for orchestrating Rapid Sterilization and stalled chronic wound regeneration. Adv Funct Mater. 2022;32(7):23.
87. Yang ZP, Fu XL, Ma DC, Wang YL, Peng LM, Shi JC, et al. Growth factor-decorated Ti3C2 MXene/MoS2 2D bio-heterojunctions with Quad-Channel Photonic disinfection for effective regeneration of Bacteria-invaded cutaneous tissue. Small. 2021;17(50):18.
88. Nuccitelli R. A role for endogenous electric fields in wound healing. In: Schatten GP, editor. Current topics in Developmental Biology. Current topics in Developmental Biology. Volume 58. 58. San Diego: Elsevier Academic Press Inc; 2003. pp. 1–.
89. Petrofsky J, Schwab E, Lo T, Cuneo M, Lawson D. The thermal effect on the blood flow response to electrical stimulation. Med Sci Monitor. 2007;13(11):CR498–CR504.
90. Ud-Din S, Sebastian A, Giddings P, Colthurst J, Whiteside S, Morris J, et al. Angiogenesis is Induced and Wound size is reduced by Electrical Stimulation in an Acute Wound Healing Model in Human skin. PLoS ONE. 2015;10(4):22.
91. Snyder AR, Perotti AL, Lam KC, Bay RC. The influence of high-voltage electrical stimulation on edema formation after Acute Injury: a systematic review. J Sport Rehabil. 2010;19(4):436–51.
92. Sebastian A, Syed F, Perry D, Balamurugan V, Colthurst J, Chaudhry IH, et al. Acceleration of cutaneous healing by electrical stimulation: degenerate electrical waveform down-regulates inflammation, up-regulates angiogenesis and advances remodeling in temporal punch biopsies in a human volunteer study. Wound Repair Regen. 2011;19(6):693–708.
93. Zhao M, Song B, Pu J, Wada T, Reid B, Tai GP, et al. Electrical signals control wound healing through phosphatidylinositol-3-OH kinase-gamma and PTEN. Nature. 2006;442(7101):457–60.
94. Reid B, Zhao M. The Electrical response to Injury: Molecular Mechanisms and Wound Healing. Adv wound care. 2014;3(2):184–201.
95. Thrivikraman G, Boda SK, Basu B. Unraveling the mechanistic effects of electric field stimulation towards directing stem cell fate and function: a tissue engineering perspective. Biomaterials. 2018;150:60–86.
96. Mao L, Hu SM, Gao YH, Wang L, Zhao WW, Fu LN, et al. Biodegradable and Electroactive regenerated bacterial Cellulose/MXene (Ti3C2Tx) composite hydrogel as Wound Dressing for accelerating skin Wound Healing under Electrical Stimulation. Adv Healthc Mater. 2020;9(19):13.
97. Kim HS, Sun X, Lee JH, Kim HW, Fu X, Leong KW. Advanced drug delivery systems and artificial skin grafts for skin wound healing. Adv Drug Deliv Rev. 2019;146:209–39.
98. Liang Y, Zhao X, Hu T, Chen B, Yin Z, Ma PX, et al. Adhesive Hemostatic conducting Injectable Composite Hydrogels with Sustained Drug Release and Photothermal Antibacterial Activity to promote full-thickness skin regeneration during Wound Healing. Small. 2019;15(12):e1900046.
99. Yang X, Zhang CQ, Deng DW, Gu YQ, Wang H, Zhong QF. Multiple stimuli-responsive MXene-Based hydrogel as Intelligent Drug Delivery Carriers for Deep Chronic Wound Healing. Small. 2022;18(5):10.
100. Hao F, Wang LY, Chen BL, Qiu L, Nie J, Ma GP. Bifunctional Smart Hydrogel dressing with strain sensitivity and NIR-Responsive performance. ACS Appl Mater Interfaces. 2021;13(39):46938–50.
101. Zhang X, Chen G, Bian F, Cai L, Zhao Y. Encoded microneedle arrays for detection of skin interstitial fluid biomarkers. Advanced materials (Deerfield Beach. Fla). 2019;31(37):e1902825.
102. Yang SY, O'Cearbhaill ED, Sisk GC, Park KM, Cho WK, Villiger M, et al. A bio-inspired swellable microneedle adhesive for mechanical interlocking with tissue. Nat Commun. 2013;4:1702.
103. Sun L, Fan L, Bian F, Chen G, Wang Y, Zhao Y. MXene-Integrated Microneedle Patches with Innate Molecule Encapsulation for Wound Healing. Research. 2021;2021:6.
104. Guo MZ, Wang YQ, Gao BB, He BF. Shark tooth-inspired Microneedle Dressing for Intelligent Wound Management. ACS Nano. 2021;15(9):15316–27.

105. Ding YP, Li W, Zhang F, Liu ZH, Ezazi NZ, Liu DF, et al. Electrospun Fibrous Architectures for Drug Delivery, tissue Engineering and Cancer Therapy. Adv Funct Mater. 2019;29(2):35.
106. Xu X, Wang SG, Wu H, Liu YF, Xu F, Zhao JL. A multimodal antimicrobial platform based on MXene for treatment of wound infection. Colloid Surf B-Biointerfaces. 2021;207:10.

Publisher's Note